Myostatin Induces Degradation of Sarcomeric Proteins through a Smad3 Signaling Mechanism During Skeletal Muscle Wasting

Sudarsanareddy Lokireddy, Craig McFarlane, Xiaojia Ge, Huoming Zhang, Siu Kwan Sze, Mridula Sharma, and Ravi Kambadur

School of Biological Sciences (S.L., X.G., H.Z., S.K.S., R.K.), Nanyang Technological University, Singapore 637551; Singapore Institute for Clinical Sciences (A*STAR) (C.M., R.K.), Brenner Centre for Molecular Medicine, Singapore 117609; and Department of Biochemistry (M.S.), Yong Loo Lin School of Medicine, National University of Singapore, MD7, Singapore 117597

Ubiquitination-mediated proteolysis is a hallmark of skeletal muscle wasting manifested in response to negative growth factors, including myostatin. Thus, the characterization of signaling mechanisms that induce the ubiquitination of intracellular and sarcomeric proteins during skeletal muscle wasting is of great importance. We have recently characterized myostatin as a potent negative regulator of myogenesis and further demonstrated that elevated levels of myostatin in circulation results in the up-regulation of the muscle-specific E3 ligases, Atrogin-1 and muscle ring finger protein 1 (MuRF1). However, the exact signaling mechanisms by which myostatin regulates the expression of Atrogin-1 and MuRF1, as well as the proteins targeted for degradation in response to excess myostatin, remain to be elucidated. In this report, we have demonstrated that myostatin signals through Smad3 (mothers against decapentaplegic homolog 3) to activate forkhead box O1 and Atrogin-1 expression, which further promotes the ubiquitination and subsequent proteasome-mediated degradation of critical sarcomeric proteins. Smad3 signaling was dispensable for myostatin-dependent overexpression of MuRF1. Although down-regulation of Atrogin-1 expression rescued approximately 80% of sarcomeric protein loss induced by myostatin, only about 20% rescue was seen when MuRF1 was silenced, implicating that Atrogin-1 is the predominant E3 ligase through which myostatin manifests skeletal muscle wasting. Furthermore, we have highlighted that Atrogin-1 not only associates with myosin heavy and light chain but also ubiquitinates these sarcomeric proteins. Based on presented data we propose a model whereby myostatin induces skeletal muscle wasting through targeting sarcomeric proteins via Smad3-mediated up-regulation of Atrogin-1 and forkhead box O1. (***Molecular Endocrinology* 25: 1936–1949, 2011**)

Cachexia is a multifactorial syndrome characterized by the progressive loss of skeletal muscle mass, with or without loss of fat mass (1, 2). The loss of protein content during skeletal muscle atrophy can be attributed to a combination of both decreased protein synthesis and increased protein degradation. Reduced genetic expression of protein synthesis components and the ubiquitin-proteasome-dependent degradation of such proteins lead to depressed protein synthesis during cachexia (3, 4). The degradation targets for the ubiquitin-proteasome pathway are not only limited to translation machinery, because the ubiquitination and the subsequent proteolysis of sarcomeric proteins are salient features of skeletal muscle wasting.

ISSN Print 0888-8809 ISSN Online 1944-9917
Printed in U.S.A.

doi: 10.1210/me.2011-1124 Received June 7, 2011. Accepted September 1, 2011.
First Published Online September 29, 2011

Abbreviations: ActRIIB, Activin receptor type 2B; CHO, Chinese hamster ovary; eiF3-f, eukaryote initiation factor 3 subunit f; Epox, Epoxomicin; FoxO1, forkhead box O1; Fstn, follistatin; GST, glutathione-*S*-transferase; HRP, horseradish peroxidase; iTRAQ, isobaric tag for relative and absolute quantification; Mstn, myostatin; MuRF1, muscle ring finger protein1; Myh, myosin heavy chain; Myl, myosin light chain; MyoD, myogenic differentiation factor; qPCR, quantitative PCR; sActRIIB, soluble ActRIIB; shRNA, short hairpin RNA; Smad, mothers against decapentaplegic homolog; TAP, tandem affinity purification.

The muscle-specific ubiquitin E3 ligases, Atrogin-1 (muscle atrophy F-box) and MuRF1 (muscle ring finger protein 1), are two important mediators of skeletal muscle atrophy (5, 6). Current literature suggests that MuRF1 specifically targets and degrades sarcomeric proteins, including myosin heavy chain (Myh) and myosin light chain (Myl), whereas Atrogin-1 ubiquitinates myogenic differentiation factor (MyoD), a promyogenic factor, and eukaryotic translation initiation factor 3 subunit F (eIF3-f), a critical component in protein translation (7, 8). The dramatic overexpression of the two E3 ligases is correlated with muscle atrophy due to immobilization, denervation, hindlimb suspension, glucocorticoid (dexamethasone) treatment, and addition of cachectic cytokines, including IL-1, IL-6, and interferon-γ (5, 9–14). The activators of Atrogin-1 and MuRF1 during skeletal muscle atrophy are FoxO1 and FoxO3, part of the FoxO family of forkhead transcription factors (5, 15). During anabolic conditions, the transcriptional activity of the FoxO proteins is suppressed by the activation of the IGF-I/phosphatidylinositol 3-kinase/Akt pathway (16, 17). However, in atrophic conditions IGF-I signaling is blocked, leading to decreased Akt activity and elevated levels of dephosphorylated, active FoxO proteins (16). Activated FoxO transcription factors induce the expression of Atrogin-1 and MuRF1, resulting in increased levels of proteasome mediated degradation (15).

Myostatin, a TGF-β superfamily member, is a secreted growth factor that acts as a potent negative regulator of muscle growth (18). Whereas the expression of a nonfunctional allele of myostatin in cattle (19) and humans (20), or the targeted disruption of myostatin in mice (21), results in severe hyperplasia and extreme muscle growth, overexpression or increased systemic levels of myostatin lead to skeletal muscle wasting (22). Myostatin-mediated skeletal muscle atrophy has been demonstrated to reduce the expression of essential myogenic regulatory factors, namely MyoD and myogenin (23, 24). In addition, along with the inhibition of myogenesis, myostatin-mediated muscle wasting results in the up-regulation of genes involved with the ubiquitin-proteasome proteolytic pathway, including Atrogin-1, MuRF1, and E214k (24).

Whereas myostatin is known to depress the activity of the IGF-I/ phosphatidylinositol 3-kinase /Akt cascade (24, 25), myostatin also elicits its catabolic effects through canonical activin receptor type-IIB (ActRIIB)/Smad (mothers against decapentaplegic homolog) signaling (26). Activated ActRIIB induces the phosphorylation of two Smad transcription factors, Smad2 and Smad3, which facilitates the expression of the FoxO transcription factors. Results from our laboratory have demonstrated that FoxO1 is required for myostatin-mediated induction of Atrogin-1 expression (24). However, whether Smad2 or Smad3 induces the expression of FoxO1 is presently unclear. In this report, we describe a mechanism whereby myostatin promotes skeletal muscle atrophy primarily through stimulating the overexpression of Atrogin-1 via the ActRIIB-Smad3-FoxO1 signaling cascade. Our data also revealed that Atrogin-1 associates with Myh and Myl and degrades them in response to myostatin treatment. Although MuRF1 was up-regulated after myostatin treatment, it assumes a secondary role when compared with Atrogin-1 in mediating myostatin-mediated skeletal muscle atrophy. Moreover, unlike Atrogin-1, MuRF1 induction during myostatin-mediated atrophy was independent of Smad3.

Results

Myostatin induces the loss of sarcomeric proteins and protein synthesis machinery during myotubular atrophy

We used an iTRAQ (isobaric tag for relative and absolute quantification)-based quantitative proteomic approach to identify proteins that were specifically degraded during myostatin-induced atrophy. The proteomic data revealed a striking reduction in the levels of several sarcomeric proteins in C2C12 myotubes treated with recombinant myostatin protein expressed and purified from *Escherichia coli* (Table 1). To identify the sarcomeric proteins that were perturbed by myostatin exposure, we homogenized and separated the insoluble fraction of the myostatin-treated C2C12 myotube protein lysate by SDS-PAGE. A single obvious difference in the protein pattern was noted in myostatin-treated myotubes when compared with untreated control myotubes (Fig. 1A). Specifically, the most abundantly stained protein (~200 kDa), which is consistent in size with Myh, was substantially reduced in myostatin-treated myotubes. In addition, we also detected a slight decrease in levels of the proteins above the 250-kDa marker; however, at this stage these proteins have not been identified (Fig. 1A). Western blot analysis was subsequently performed to validate whether Myh protein expression was reduced in response to myostatin treatment. According to Fig. 1, B and C, a pan-specific antibody detecting "fast" Myh isoforms (Myh1, Myh2, and Myh4, found in "type II" or "fast-twitch" fibers) and antibodies specific for fast 2A and fast 2B Myh revealed a marked reduction in the expression of fast Myh isoforms in C2C12 myotubes exposed to myostatin. Similarly, Western blot analysis detecting the single "slow" isoform of Myh (Myh7, found in "type I" fibers) and all isoforms of Myl revealed a comparable decrease after myostatin treatment (Fig. 1, B

TABLE 1. Sarcomeric proteins and protein synthesis machinery were significantly down-regulated upon myostatin treatment as identified by iTRAQ labeling followed by nano-liquid chromatorgraph tandem mass spectrometry

Function	Gene symbol and name	Fold inhibition	*P* value
Sarcomeric proteins	Actn3, α-actinin-3	0.425	0.003
	Des, Desmin	0.501	0.000
	Mybph, myosin-binding protein H	0.685	0.046
	Myh1, myosin-1	0.608	0.019
	Myh2, myosin, heavy polypeptide 2, skeletal muscle, adult	0.780	0.006
	Myh3, Myosin-3	0.200	0.005
	Myh4, Myosin-4	0.235	0.032
	Myh7, Myosin-7	0.525	0.035
	Myh7b, Myosin-7B	0.235	0.012
	Myh8, myosin-8	0.515	0.036
	Myh9, myosin-9	0.472	0.051
	Myl1, Myl1 protein	0.673	0.051
	Myl4, myosin light chain 4	0.457	0.006
	Mylpf, myosin regulatory light chain 2, skeletal muscle isoform	0.586	0.010
	Tnnc2, troponin C, skeletal muscle	0.056	0.003
	Tnni1, troponin I, slow skeletal muscle	.567	0.012
	Ttn, isoform 1 of Titin	0.394	0.000
Protein synthesis machinery	Eif3f, eukaryotic translation initiation factor 3 subunit F	0.526	0.025
	Eef2, elongation factor 2	0.667	0.008
	Eif3a, eukaryotic translation initiation factor 3 subunit A	0.278	0.020
	Eif3k, isoform 1 of eukaryotic translation initiation fact 3 subunit K	0.759	0.031
	Eif4g2, eukaryotic translation initiation factor 4, γ 2 form 1	0.625	0.036
	Eif5b, isoform 1 of eukaryotic translation initiation factor 5B	0.698	0.041
	Rps4, ×40S ribosomal protein S4, X isoform	0.350	0.008
	Rps3, 40S ribosomal protein S3	0.575	0.012
	Rpsa, ribosomal protein SA	0.643	0.028
	Rps24, isoform 3 of 40S ribosomal protein S2	0.673	0.011
	Rps11, 40S ribosomal protein S11	0.643	0.012

The values were normalized to 1 by relative abundance of proteins found in two duplicates from two independent experiments.

and C). Next, we determined whether the changes in Myh and Myl protein expression during myostatin-induced atrophy could be attributed to the alterations of their respective mRNA levels as opposed to an increase in protein turnover. Real-time quantitative PCR (qPCR) analysis of mRNA levels of the five distinct Myh and three unique Myl isoforms indicated that myostatin treatment did not significantly alter the mRNA expression of the myosin isoforms, hence confirming that the decreased Myh and Myl protein levels were due to posttranscriptional events including protein translation (Fig. 1D). These observations are also consistent with the iTRAQ data, which highlighted the reduced levels of several proteins involved in protein synthesis in C2C12 myotubes treated with myostatin (Table 1). Therefore, we next assessed the effect of myostatin (Mstn) on protein synthesis in C2C12 myotubes. The results clearly suggest that, treatment with myostatin reduced protein synthesis in myotubes (Fig. 1G).

The muscle-specific E3 ligases, Atrogin-1 and MuRF1, are central to skeletal muscle atrophy. During myostatin-mediated atrophy in C2C12 myotubes, we observed the elevation of mRNA and protein levels of both Atrogin-1 and MuRF1 (Fig. 1, B, C and F). Treating C2C12 myotubes with conditioned medium from Chinese hamster ovary (CHO) cells, engineered to overexpress and secrete the functional myostatin protein (22), manifested a myotubular wasting phenotype similar to that observed after addition of recombinant myostatin protein purified from *E. coli*. Specifically, we observed reduced myotube area (data not shown), decreased protein levels of Myh and Myl, and increased expression of Atrogin-1 and MuRF1 (Fig. 1E).

Previously it has been shown that soluble ActRIIB (sActRIIB) and follistatin (Fstn) inhibit myostatin signaling (27–29). Therefore, we performed real-time qPCR to monitor the levels of *Atrogin-1* and *MuRF1* and found that treatment with sActRIIB and follistatin inhibited myostatin-mediated induction of *Atrogin-1* and *MuRF1* expression in C2C12 myotubes (Fig. 1F). These results taken together suggest that myostatin induces myotubular atrophy through not only decreasing the protein synthesis, but also by up-regulating the expression of muscle-specific E3 ligases.

Myostatin treatment results in increased ubiquitination and proteasome-dependent degradation of sarcomeric proteins

To confirm whether myostatin-mediated degradation of sarcomeric proteins occurs via the ubiquitination sys-

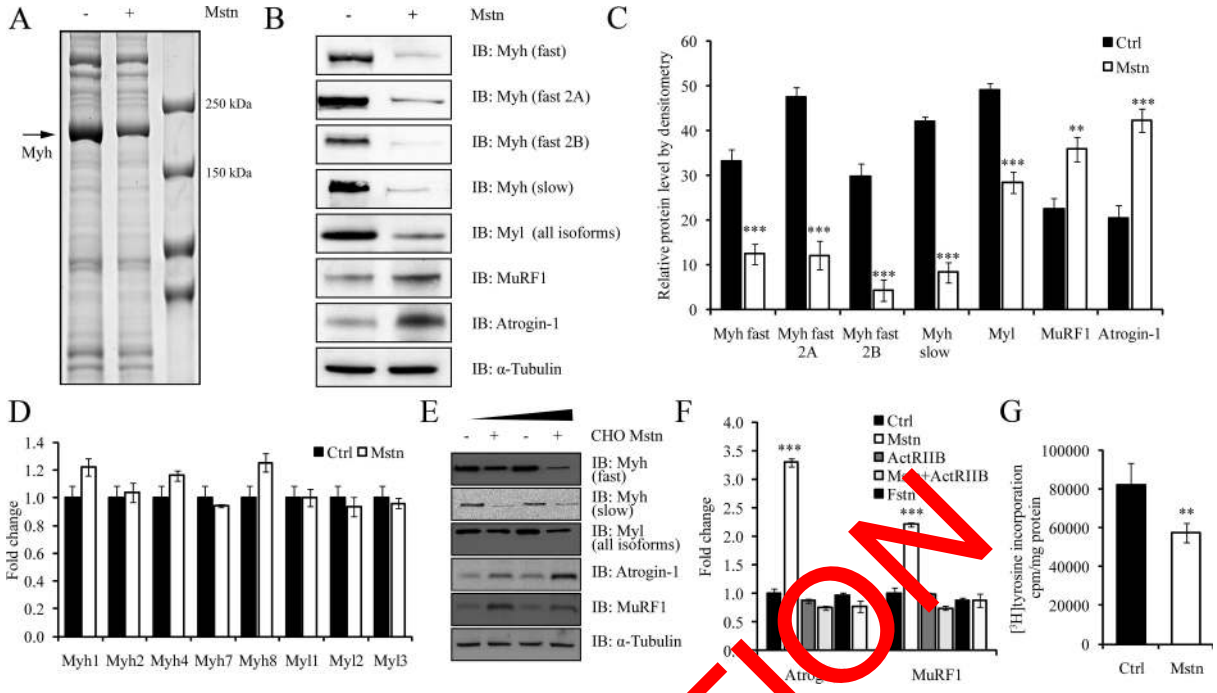

FIG. 1. Myostatin induces the loss of sarcomeric proteins and protein synthesis machinery during myotubular atrophy. A, A micrograph showing a Coomassie blue-stained SDS-PAGE. The molecular weight marker is indicated in lane 3 (from *left*). Protein lysates from myostatin treated (+) or untreated myotubes (−) are shown. The *arrow* indicates an approximately 200-kDa protein which is reduced after myostatin treatment. The molecular mass (kDa) of the protein is similar to that of Myh. B, Analysis of Myh and Myl isoforms by immunoblotting (IB). *First panel*, Myh fast type 2 isoforms; *Second panel*, Myh fast 2A; *Third panel*, Myh fast 2B, *fourth panel*, Myh slow; and *fifth panel*, Myl (all isoforms). The *sixth* and *seventh* panels refer to MuRF1 and Atrogin-1, respectively. The levels of α-tubulin were assessed to ensure equal loading. C, Densitometric analysis of Myh (all isoforms), Myl (all isoforms), MuRF1, and Atrogin-1. $P < 0.01$ (**) and $P < 0.001$ (***) and *error bars* represent the mean ± SD from three replicate experiments. D, Real time-qPCR analysis of individual isoforms of *Myh* and *Myl* from untreated (Ctrl) and myostatin-treated (Mstn) myotubes. E, Differentiated C2C12 myotubes were treated with conditioned media containing eukaryotic produced CHO-cell secreted myostatin (10 and 20 ng, as estimated by ELISA) with the protein extracts subjected to IB analysis with Myh fast antibody (*first panel*), Myh slow antibody (*second panel*), and an antibody that detects all isoforms of Myl (*third panel*). The *fourth and fifth panels* depict Atrogin-1 and MuRF1 protein levels, respectively. The levels of α-tubulin were assessed to ensure equal loading. F, Real time-qPCR analysis of mRNA expression of *Atrogin-1 and MuRF1* in the presence or absence of recombinant myostatin (Mstn), soluble ActRIIB (ActRIIB) and follistatin (Fstn). The *graph* depicts the mean fold change in gene expression and is representative of triplicate experiments. $P < 0.001$ (***) and *error bars* represent the mean ± SD. G, Mstn suppresses protein synthesis in differentiated myotubes. After 24 h of treatment with Mstn, myotubes were incubated with [^{3}H]tyrosine for 2 h. The radioactivity incorporated was measured and normalized to total protein lysate. $P < 0.01$ (**), and *error bars* represent the mean ± SD. Ctrl, Control.

tem, sarcomeric proteins found in the insoluble fraction of control or myostatin-treated C2C12 myotube protein lysates were subjected to Western blot analysis with a pan-ubiquitin-specific antibody (Fig. 2A). The Western blot and corresponding densitometric analysis indicated significantly elevated amounts of protein ubiquitination in myostatin-treated myotubes when compared with the control (Fig. 2B). These results indicate that excess myostatin induces extensive ubiquitination of sarcomeric proteins. Next, we tested whether blocking proteasome function would rescue myostatin-mediated Myh and Myl degradation. Two proteasome inhibitors, MG132 and Epoxomicin (Epox), are known to curtail proteasome-mediated protein turnover and thereby increase protein content during muscle atrophy (7, 9, 30). Therefore, C2C12 myotubes were treated with myostatin in the presence or absence of either MG132 or Epox, and the levels of various isoforms of Myh and Myl were analyzed by immunoblotting (Fig. 2, C and D). Whereas myostatin treatment resulted in the loss of both fast and slow isoforms of Myh and Myl, the addition of either MG132 or Epox, however, blocked myostatin-mediated protein degradation (Fig. 2, C and D). Importantly, the levels of Myh and Myl in C2C12 myotubes exposed to myostatin remained comparable to untreated control, in the presence of the proteasome inhibitors, despite increased expression of Atrogin-1 and MuRF1 (Fig. 2, C and D). In addition, analysis of protein degradation, as measured by the percentage of [^{3}H]tyrosine lost after myostatin treatment, demonstrated elevated levels of protein turnover when compared with the control (Fig. 2E). Moreover, the increased level of proteolysis was blocked by addition of MG132 (Fig. 2E).

Myostatin-induced sarcomeric protein degradation occurs preferentially through Atrogin-1

The results thus far indicate that myostatin treatment induces the expression of two major ubiquitin E3 ligases,

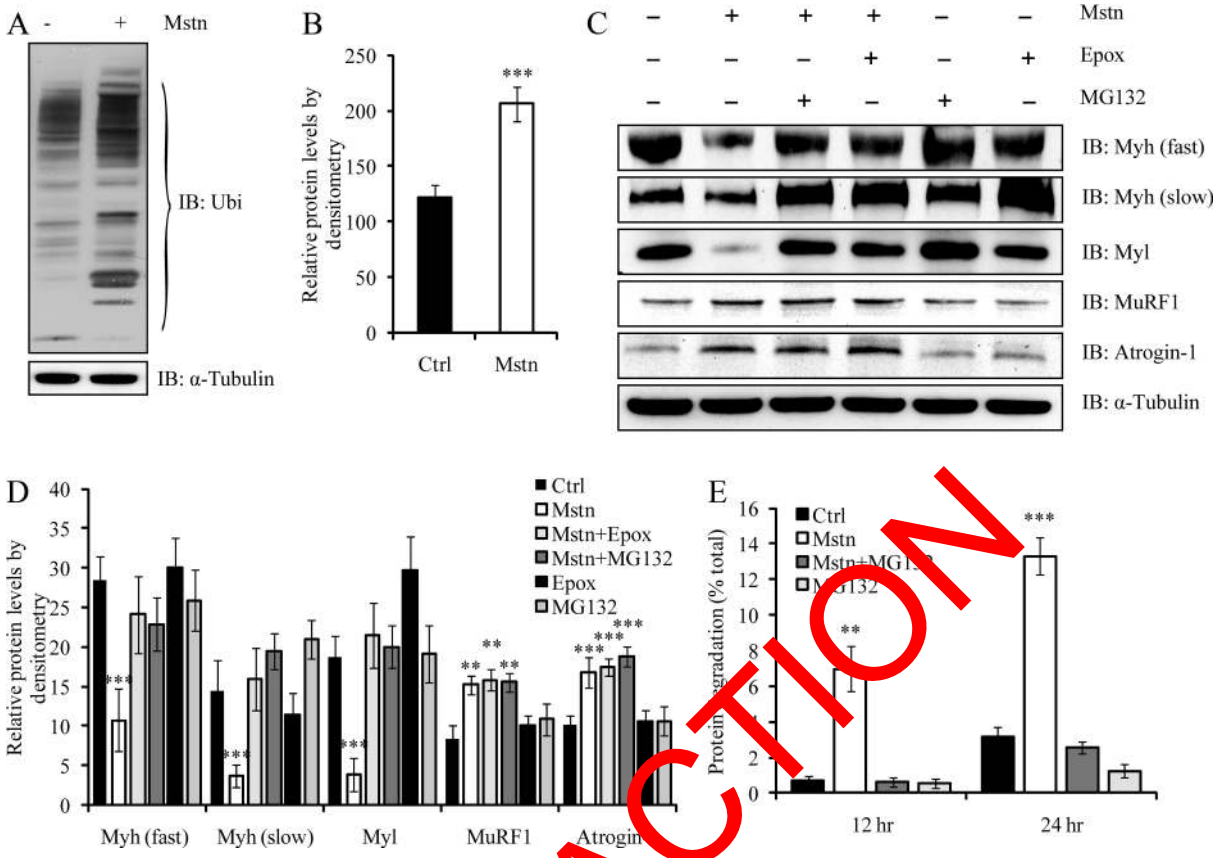

FIG. 2. Myostatin treatment results in increased ubiquitination and proteasome-dependent degradation of sarcomeric proteins. C2C12 myotubes were differentiated and treated with myostatin. A, Sarcomeric protein enriched fraction was analyzed by immunoblotting using specific anti-ubiquitin (Ubi) antibodies. The *top panel* displays total ubiquitinated proteins in myostatin treated (+) and untreated (−) protein lysates. The levels of α-tubulin were assessed to ensure equal loading. B, Densitometric analysis of ubiquitinated proteins, displayed as mean relative protein level from two replicate experiments. $P < 0.001$ (***) and the *error bars* represent mean of ± SD. C, Immunoblotting (IB) analysis of Myh isoforms (fast and slow), Myl (all isoforms), MuRF1, and Atrogin-1 after treatment with (+) or without (−) myostatin in the presence (+) or absence (−) of either Epox or MG132. The levels of α-tubulin were assessed to ensure equal loading. D, Densitometry analysis of IB for Myh (fast and slow), Myl (all isoforms), Atrogin-1, and MuRF1, normalized to α-tubulin. The *error bars* represent mean ± SD from three independent experiments. E, Myostatin increases proteolysis in differentiated myotubes. Differentiated myotubes were incubated with [^{3}H]tyrosine for 36 h and then treated with Mstn or MG132 or a combination of both. Media were collected at 12 and 24 h, and the amount of degraded [^{3}H]tyrosine-labeled protein was expressed as a percentage of the initial amount of [^{3}H]tyrosine added. Statistical significance was assessed. $P < 0.01$ (**) and $P < 0.001$ (***). Ctrl, Control.

Atrogin-1 and MuRF1, to promote protein degradation. However, the individual contribution of Atrogin-1 and MuRF1 in myostatin-mediated skeletal muscle atrophy has yet to be studied. To address this question in further detail, C2C12 myotubes stably overexpressing short hairpin RNA (shRNA) designed to specifically target and inhibit either Atrogin-1 (shAtrogin-1) or MuRF1 (shMuRF1) were generated. Using real time qPCR, we identified that shRNA overexpression resulted in the down-regulation of *Atrogin-1* and *MuRF1* mRNA expression levels to 80% of that observed in control myotubes, confirming that the shRNA was effective in reducing the levels of the target mRNA (Fig. 3, A and B). The real time qPCR analysis also validated that the reduction in mRNA is specific to the respective shRNA expressed, because we did not observe a decrease in the levels of *Atrogin-1* mRNA in myotubes that expressed *MuRF1* shRNA and vice versa (Fig. 3, A and B).

Given the specificity and efficiency of the Atrogin-1 and MuRF1 shRNA, the protein level of Myh and Myl in C2C12 extracts treated myostatin was then examined (Fig. 3C). Western blot and densitometric analysis revealed that Atrogin-1 knockdown resulted in the loss of approximately 20–30% of Myh and Myl expression upon myostatin treatment. Conversely, about 70–80% loss of Myh and Myl expression was noted when MuRF1 was silenced (Fig. 3, C and D). As expected, in the presence of scrambled shRNA (shCon), myostatin treatment yielded an increase in the expression of both Atrogin-1 and MuRF1, and a decrease in both Myh and Myl protein levels (Fig. 3, C and D). In contrast, shRNA-mediated knockdown of either Atrogin-1 or MuRF1 prevented myostatin-dependent up-regulation of Atrogin-1 and MuRF1, respectively (Fig. 3C).

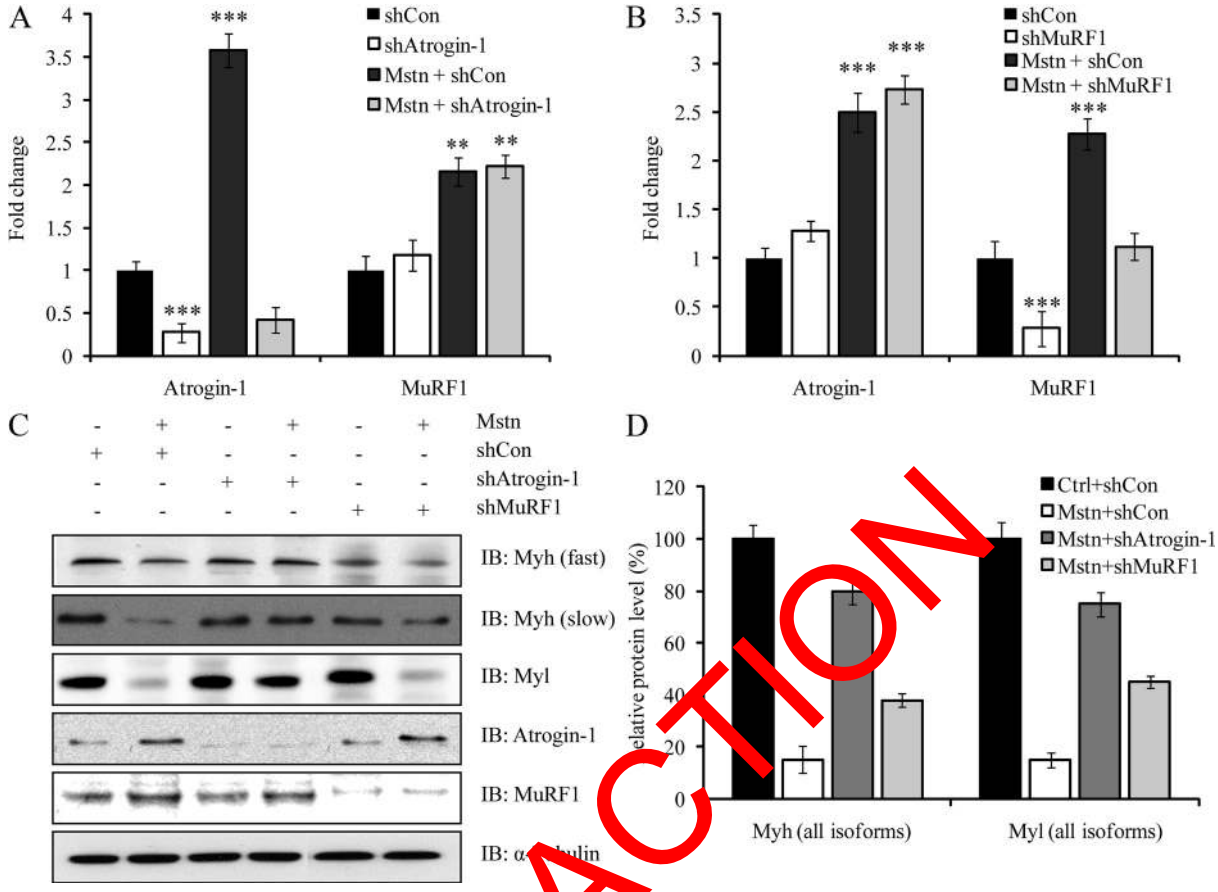

FIG. 3. Myostatin-induced sarcomeric protein degradation occurs differentially through Atrogin-1. Myoblasts were transfected with control shRNA (shCon) or shAtrogin-1 or shMuRF1 expressing *silencer* constructs. Stable knockdown myotube cultures were differentiated for 3 d and treated with (+) or without (−) myostatin. A, Real time-qPCR analysis of *Atrogin-1* and *MuRF1* expression in Atrogin-1 knockdown cells after myostatin treatment. B, Real time-qPCR analysis of *Atrogin-1*, and *MuRF1* expression in MuRF1 knockdown cells after myostatin treatment. *Graphs* display mean fold changes and are representative of three replicate plates. Each mRNA expression level was determined relative to the mean expression level of mRNA in control cells. $P < 0.01$ (**), $P < 0.001$ (***), and *error bars* represent ± SD. C, Immunoblotting (IB) analysis of Atrogin-1, MuRF1, Myh (fast and slow) and Myl expression in Atrogin-1 and MuRF1 shRNA knockdown cells after treatment with (+) or without (−) myostatin. The levels of α-tubulin were assessed to ensure equal loading. D, Densitometric analysis of IB for Myh and Myl isoforms after treatment with or without myostatin (Mstn) in shCon-, shAtrogin-1-, and shMuRF1-transfected myotubes. The relative protein level (%) was calculated by normalizing the control (shCon) to 100%. The data have been generated from four independent experiments. *Error bars* represent mean ± SD. Ctrl, Control.

To confirm that the changes in sarcomeric protein levels were not due to alterations in the mRNA, the expression of Myh and Myl isoforms was determined by real time qPCR using RNA from Atrogin-1 and MuRF1 knockdown myotubes (Supplemental Fig. 1, published on The Endocrine Society's Journals Online web site at http://mend.endojournals.org). The mRNA expression level of *Myh1*, *Myh2*, *Myh4*, *Myh7*, *Myh8* *Myl1*, *Myl2*, and *Myl3* did not change significantly with Atrogin-1 and MuRF1 shRNA transfection when compared with shCon-transfected myotubes (Supplemental Fig. 1), further suggesting that the depression of sarcomeric proteins can be attributed to posttranscriptional events.

To further verify the central role of Atrogin-1 in myostatin-mediated degradation of sarcomeric proteins, primary myotubes from Atrogin-1 knockout mice (Atrogin-$1^{-/-}$) and wild-type (Atrogin-$1^{+/+}$) mice were cultured and treated with myostatin, and protein extracts were subjected to Western blotting. According to Fig. 4A, there was no significant degradation of Myh (Fast and Slow) and Myl isoforms in Atrogin-$1^{-/-}$ myotubes after myostatin treatment, even though a significant up-regulation of MuRF1 was observed (Fig. 4A). Consistent with this result, myostatin treatment of Atrogin-$1^{-/-}$ myotube cultures did not result in any significant myotubular wasting, as measured by myotube area (Fig. 4B). Furthermore, we measured the levels of MyoD in Atrogin-$1^{-/-}$ primary myotubes and found that MyoD protein expression did not change significantly in Atrogin-$1^{-/-}$ myotubes when compared with wild-type myotubes challenged with myostatin (data not shown).

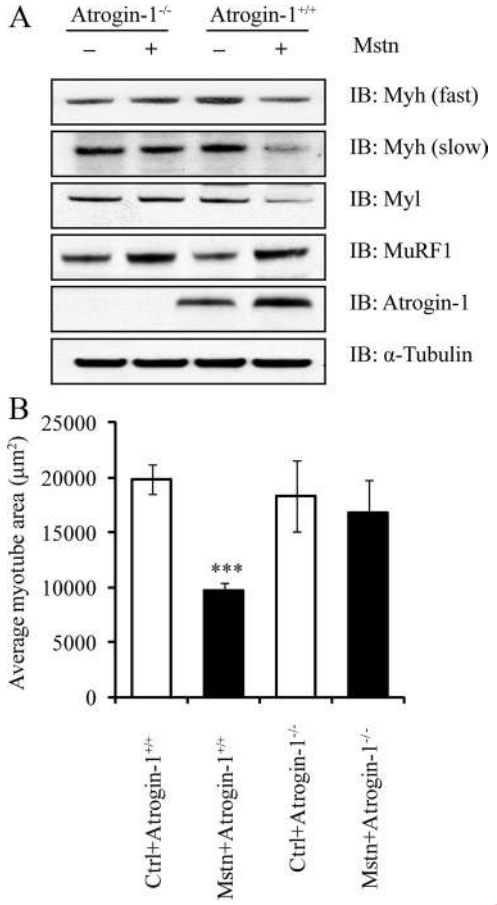

FIG. 4. Myostatin-induced myotubular atrophy and degradation of sarcomeric proteins is abrogated in Atrogin-1 knockout primary myotubes. A, Immunoblotting (IB) analysis of Myh isoforms (fast and slow), Myl, Atrogin-1, and MuRF1 in Atrogin-1$^{-/-}$ and Atrogin-1$^{+/+}$ myotubes treated with (+) or without (−) myostatin (Mstn). The levels of α-tubulin were assessed to ensure equal loading. B, Quantification of average myotube area (μm^2) in wild-type (Atrogin-1$^{+/+}$) and Atrogin-1-null mice (Atrogin$^{-/-}$) after treatment with myostatin. *Graph* represents the average myotube area (μm^2) analyzed per genotype, across 20 images from two coverslips from two independent experiments. $P < 0.001$(***) and *error bars* represent mean ± SD. Ctrl, Control.

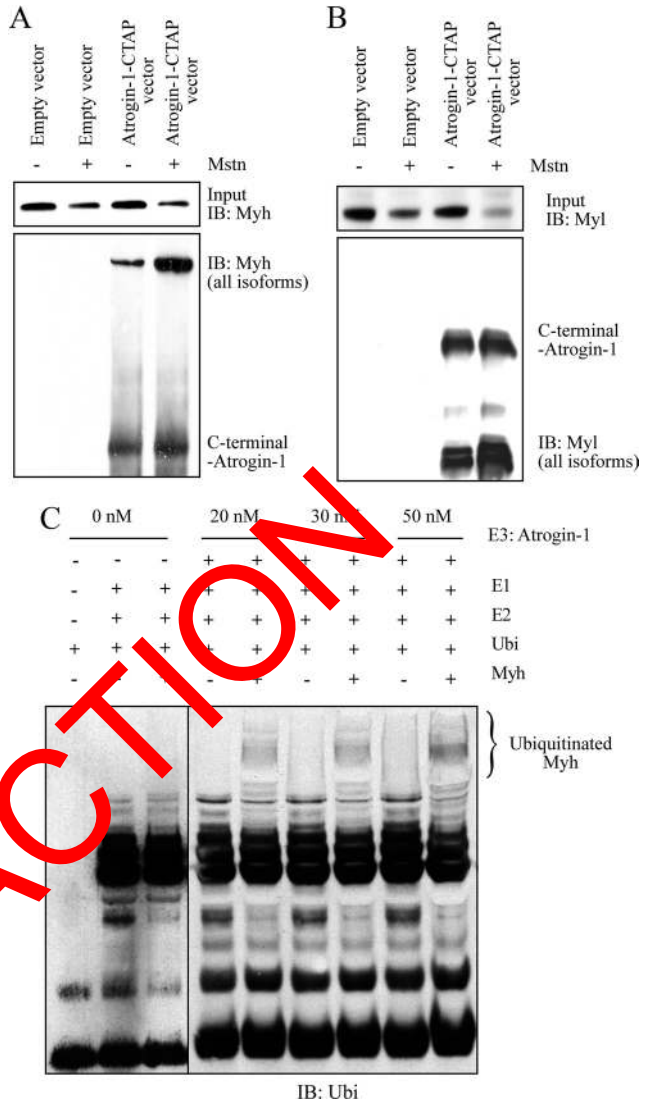

FIG. 5. Myosin heavy and light chain proteins are physically associated with Atrogin-1 and are ubiquitinated by Atrogin-1 *in vitro*. A and B, Coimmunoprecipitation (Co-IP) analysis of CTAP-labeled Atrogin-1 (Atrogin-1-CTAP) in the presence (+) or absence (−) of recombinant myostatin protein. Myh and Myl were detected using the antibodies against Myh (all isoforms) and Myl (all isoforms). C, To study *in vitro* ubiquitination, Myh (1 μM) was incubated with increasing concentrations (0 nM, 20 nM, 30 nM, and 50 nM) of GST-hAtrogin-1 for 1 h. Immunoblotting (IB) analysis with an anti-ubiquitin (Ubi) antibody is shown. Ubiquitinated Myh band is indicated *within the brackets*.

Atrogin-1 physically associates and ubiquitinates sarcomeric proteins *in vitro*

Although MuRF1 ubiquitinates and targets sarcomeric proteins for degradation, it is currently unclear whether or not Atrogin-1 performs a similar function during myostatin-induced skeletal muscle wasting. Thus, we determined whether myostatin treatment increases the physical association between Atrogin-1 and sarcomeric proteins by performing tandem affinity purification (TAP) (Fig. 5A and B). According to Fig. 5, A and B, myostatin treatment on C2C12 myotubes expressing the empty vector (control) resulted in reduced levels of both Myh and Myl. Whereas similar sarcomeric protein loss was observed when C2C12 myotubes expressing Atrogin-1-CTAP vector were exposed to myostatin, the coimmunoprecipitated complex revealed that myostatin treatment increased Myh/Myl-Atrogin-1 association (Fig. 5, A and B). It is noteworthy to mention that Myh and Myl also associated with Atrogin-1 in the untreated samples, which is most likely due to the constitutive expression of Atrogin-1 under normal physiological conditions (Fig. 5, A and B). Next we performed an *in vitro* ubiquitination assay to confirm whether or not sarcomeric proteins are substrates for Atrogin-1 ubiquitin ligase activity. Results demonstrated that increasing concentrations of glutathione-*S*-transferase (GST)-hAtrogin-1 corresponded to increased levels of ubiquitinated Myh

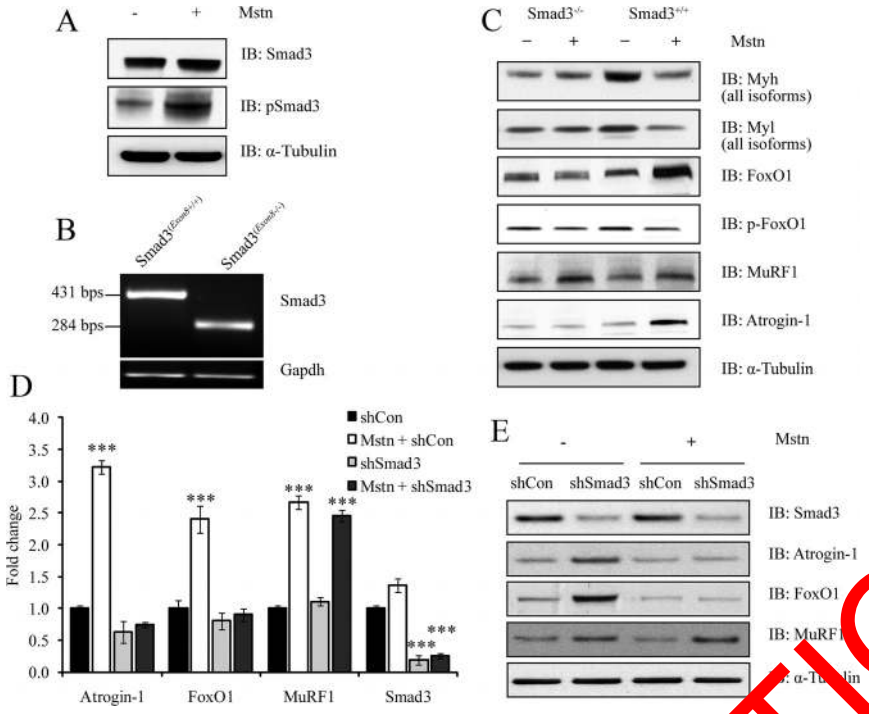

FIG. 6. Myostatin induces skeletal muscle atrophy by up-regulating FoxO1 and Atrogin-1 (but not MuRF1) through a Smad3-dependent signaling mechanism. A, Immunoblotting (IB) analysis of Smad3 and pSmad3 after treatment with (+) or without (−) myostatin in C2C12 myotubes. The levels of α-tubulin were assessed to ensure equal loading. B, real-time qPCR analysis was used to detect the truncated allele (*Exon8*) of Smad3 in Smad3$^{-/-}$ and Smad3$^{+/+}$ primary myoblasts. The expression of *Gapdh* was assessed to ensure that equal amount of template was used in PCR. C, IB analysis of Myh (all isoforms), Myl (all isoforms), FoxO1, p-FoxO1, MuRF1, and Atrogin-1 in primary myotube cultures from Smad3-null (Smad3$^{-/-}$) and wild-type (Smad3$^{+/+}$) mice, after treatment with (+) or without (−) recombinant myostatin protein (Mstn). The levels of α-tubulin were assessed to ensure equal loading. D, The real time-qPCR analysis of *Atrogin-1*, *FoxO1*, *MuRF1*, and *Smad3* expression after shRNA-mediated Smad3 knockdown (shSmad3) and myostatin (Mstn) treatment. *Graph* represents mean relative fold changes and is indicative of three replicate experiments. Each mRNA expression level was determined relative to the mean expression level of that mRNA in shCon cells. $P < 0.001$ (***) and the *error bars* represent ± SD. E, IB analysis of Smad3, Atrogin-1, FoxO1, and MuRF1 proteins in Smad3 knockdown (shSmad3) C2C12 myotubes treated with or without myostatin. The levels of α-tubulin were assessed to ensure equal loading of protein.

(Fig. 5C). However, no ubiquitinated Myh band was observed in the absence of Atrogin-1 (Fig. 5C). Collectively, these results confirm that Atrogin-1 can directly associate and ubiquitinate Myh.

Myostatin induces atrophy by up-regulating FoxO1 and Atrogin-1 through a Smad3-dependent signaling mechanism

Treatment with myostatin increased Smad3 phosphorylation in myotubes (Fig. 6A). To analyze whether the Smad3-signaling pathway plays a dominant role during myostatin-mediated skeletal muscle atrophy, we cultured and differentiated primary myotubes from wild-type (Smad3$^{+/+}$) and Smad3 null (Smad3$^{-/-}$) mice, and treated with myostatin. Expression of mutant Smad3 allele in the myotubes isolated from Smad3 null muscles is shown in Fig. 6B. Total proteins were then extracted, and immunoblotting was performed to analyze the expression of Myh (all isoforms), Myl (all isoforms), Atrogin-1, MuRF1, FoxO1, and p-FoxO1. As expected, treatment with myostatin resulted in the significant up-regulation of Atrogin-1, MuRF1, and FoxO1 protein expression in Smad3$^{+/+}$ myotubes (Fig. 6C). Importantly, although MuRF1 was also up-regulated in Smad3$^{-/-}$ myotubes after addition of myostatin, myostatin failed to induce the expression of Atrogin-1 and FoxO1 in the absence of Smad3 (Fig. 6C). In addition to the primary cultures, we have repeated this experiment in C2C12 myotubes overexpressing shRNA designed to specifically target and repress Smad3 levels (Fig. 6, D and E). By real time qPCR analysis, we found that whereas there is a significant increase in the expression of *Atrogin-1* and *FoxO1* upon myostatin treatment in control C2C12 cells, down-regulation of Smad3 results in the abrogation of myostatin-mediated induction of *Atrogin-1* and *FoxO1* (Fig. 6D). In contrast, expression of *MuRF1* continued to be up-regulated by myostatin despite Smad3 silencing (Fig. 6D). Consistent with gene expression data, Western blot analysis confirmed that myostatin requires Smad3 protein for the up-regulation of Atrogin-1 (Fig. 6E). This observation was consistent with the primary culture data mentioned above and clearly suggests that even though myostatin requires Smad3 signaling to regulate *Atrogin-1* and *FoxO1* gene expression, Smad3 signaling is dispensable for myostatin-mediated up-regulation of MuRF1.

Discussion

An increase in circulating levels of myostatin results in cachectic-like muscle wasting (22, 24, 31). The up-regulation of myostatin ablates the expression of several contractile proteins in skeletal muscle (23, 32). Using the murine myoblast system and recombinant myostatin protein, we have recently demonstrated that myostatin induces skeletal muscle wasting by elevating the expression

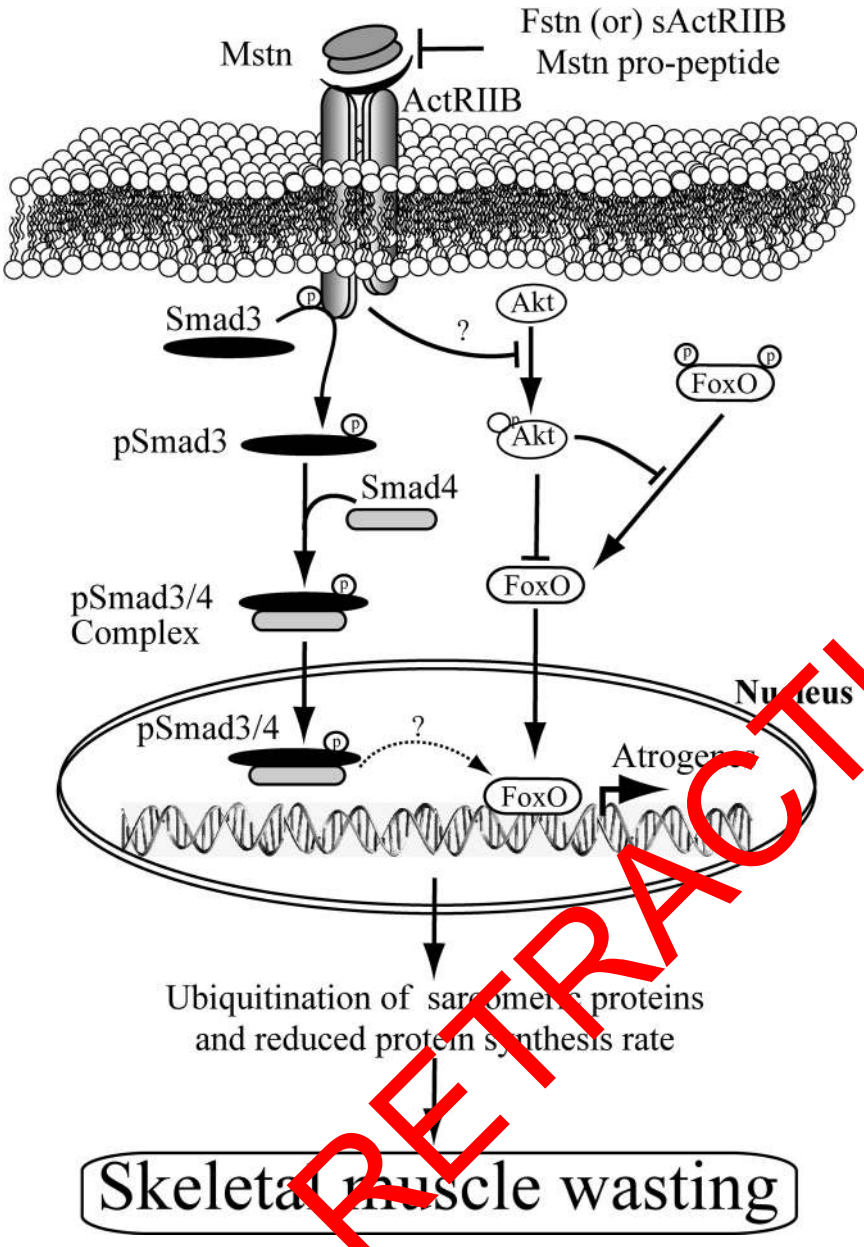

FIG. 7. Mechanism of myostatin-induced skeletal muscle atrophy. Proposed mechanism behind myostatin-induced skeletal muscle wasting. Myostatin up-regulates components of ubiquitin proteolysis system, including Atrogin-1, through a FoxO1- and Smad3-dependent signaling mechanism. Enhanced activation of the ubiquitination system leads to degradation of the majority of sarcomeric proteins, which are required for normal muscle growth and development. Myostatin also inhibits protein synthesis by decreasing the phosphorylation of Akt and reduced protein synthesis machinery, leading to enhanced progression of skeletal muscle atrophy. Importantly, myostatin-induced skeletal muscle atrophy is reversible, as shown through the action of its known antagonists, including soluble ActRIIB and follistatin (Fstn). *Arrows* (→) represent activation, whereas *blunt-ended* (⊥) *lines* represent inhibition.

of numerous components of the ubiquitin-proteasome pathway, including the muscle-specific E3 ligases, Atrogin-1 and MuRF1 (24, 33). In this report, we have presented several lines of evidence to conclude that myostatin induces muscle wasting by not only inhibiting protein synthesis but also by inducing the ubiquitin-proteasome-dependent degradation of C2C12 myotube sarcomeric proteins. We have highlighted that Atrogin-1 is the foremost muscle-specific E3 ligase that facilitates myostatin-mediated muscle wasting, and that regulation of the Atrogin-1 is controlled by the ActRIIB-Smad3-FoxO1 signaling axis (Fig. 7).

Proteomic data demonstrated that several proteins involved in translation, thick and thin filament proteins, were degraded when myotubes were treated with myostatin (Table 1). A Coomassie-stained gel comparing protein lysates enriched with sarcomeric proteins from control and myostatin-treated myotubes further highlighted that a single protein, consistent in molecular weight with Myh, was highly abundant in control myotubes but reduced in lysates from myostatin-treated myotubes (Fig. 1A). Subsequent immunoblot analysis confirmed that this particular protein was Myh (Fig. 1B). Furthermore, myostatin treatment of C2C12 myotubes resulted in the indiscriminate proteolysis of both slow and fast Myh (2A, 2B) isoforms (Fig. 1, B and C). Because there was no change in mRNA levels of Myh and Myl isoforms (Fig. 1D), we concluded that the reduced levels of the various myofibrillar proteins (Fig. 1B) could be due to posttranscriptional events including protein translation. Accordingly, we assessed the effect of myostatin on protein synthesis and proteosomal mediated degradation of intracellular proteins.

The increased levels of ubiquitinated sarcomeric proteins enriched in the insoluble fraction of myostatin-treated C2C12 protein lysates (Fig. 2, A and B), and the abrogation of myostatin-dependent decrease in Myh content in the presence of proteasome inhibitors (Fig. 2, C–E), substantiated the central role of the ubiquitin-proteasome pathway in the selective targeting and removal of sarcomeric proteins during myostatin-mediated atrophy (Fig. 2, C–E). Studies have established that two muscle-specific E3 ligases, Atrogin-1 and MuRF1, facilitate muscle atrophy by ubiquitinating structural and intracellular proteins for degradation (3, 4,

7, 8, 34). During myostatin-mediated C2C12 atrophy, we observed the striking up-regulation of both Atrogin-1 and MuRF1, further implicating the ubiquitin-proteasome pathway in manifesting this particular form of skeletal muscle wasting. The individual contribution of these two E3 ligases toward myostatin-mediated muscular atrophy, however, is currently unclear. Targeted shRNA-mediated inhibition of either Atrogin-1 or MuRF1 in C2C12 myotubes exposed to myostatin yielded two significant observations. First, Atrogin-1 is the principal E3 ligase that induces the majority of sarcomeric protein degradation during myostatin-mediated muscle atrophy, because the silencing of Atrogin-1 resulted in approximately 80% rescue of sarcomeric protein (Myh and Myl) expression after treatment with myostatin (Fig. 3D). Furthermore, myostatin treatment of primary myotube cultures generated from Atrogin-1 knockout mice failed to induce a significant loss of both Myh and Myl, further validating the importance of Atrogin-1 in facilitating myostatin-mediated atrophy (Fig. 4A). Second, although MuRF1 is activated in response to myostatin signaling, it does not play a major role in myostatin-induced skeletal muscle atrophy, because only about 20% of sarcomeric protein expression was rescued in the presence of MuRF1-specific shRNA (Fig. 3D).

Considering the extensive rescue of myostatin-mediated sarcomeric protein loss in the absence of Atrogin-1, we examined whether Atrogin-1 itself could target the degradation of Myh and Myl through the ubiquitin-proteasome pathway. Indeed, coimmunoprecipitation of Atrogin-1 using TAP revealed a previously unappreciated association of Myh and Myl with Atrogin-1 (Fig. 5, A and B). During myostatin-mediated atrophy, the amount of Myh and Myl associated with Atrogin-1 was markedly greater than the untreated C2C12 myotube extracts (Fig. 5, A and B), suggesting that Atrogin-1, much like MuRF1, may target sarcomeric proteins for degradation. Moreover, an *in vitro* ubiquitination assay further confirmed that Myh is directly ubiquitinated by Atrogin-1 (Fig. 5C). Taken together, these data reveal that sarcomeric proteins associate with Atrogin-1, are ubiquitinated, and finally targeted for degradation in response to myostatin treatment.

To date, Atrogin-1 has only been shown to degrade MyoD and eIF3-f in skeletal muscles (3, 35). iTRAQ proteomic data specifically confirmed the degradation of several proteins involved in protein synthesis, including eIF3-f, due to myostatin exposure (Table 1). Consistent with this we observed a decrease in protein synthesis in myotubes treated with myostatin. Trendelenburg *et al.* (25) also recently observed that myostatin treatment restricts protein synthesis, however, not by inducing Atrogin-1 but by impairing Akt/mTOR/p70S6K signaling. However, the near-complete rescue of myostatin-mediated sarcomeric protein loss during Atrogin-1 deficiency would suggest that myostatin-dependent inhibition of the Akt/mTOR/p70S6K pathway assumes a nominal role in skeletal muscle atrophy (Fig. 4A). Thus, taking into account that Atrogin-1 targets both eIF3-f and Myh for ubiquitin-mediated proteolysis, myostatin-mediated muscle atrophy is principally due to the removal of sarcomeric proteins, and decreased protein synthesis is due to the proteolysis of translation machinery (3, 4). Whether depressed Myh protein expression during myostatin-mediated atrophy is primarily due to Atrogin-1-mediated degradation of sarcomeric proteins or through Atrogin-1 promoting the degradation of protein synthesis components, like eIF3-f, is unknown.

After establishing the prominence of Atrogin-1 in facilitating myostatin-mediated muscle atrophy, we next examined the upstream signals that induce Atrogin-1 expression. Myostatin binds to ActRIIB, which in turn results in the phosphorylation of Smad2 and Smad3 (Fig. 6A) (25, 26, 37). The activated Smad transcription factors themselves induce FoxO1 and FoxO3 expression, which in turn leads to the expression of the muscle-specific E3 ligases. In this report, we show that either selective inhibition or genetic inactivation of Smad3 prevents myostatin-mediated increase in FoxO1 and corresponding Atrogin-1 expression (Fig. 6, C–E). Thus, Smad3 is an indispensable link tethering myostatin signal transduction to Atrogin-1 expression during myostatin-mediated skeletal muscle wasting (Fig. 6, C–E). These results further corroborate a recent publication by Sartori *et al.* (36), who showed that Smad3 signaling is required for the up-regulation of Atrogin-1 promoter by myostatin. MuRF1 expression, like Atrogin-1, was consistently up-regulated during myostatin-mediated muscle atrophy. However, in contrast to the data presented by Trendelenburg *et al.* (25) and Sartori et al. (36), the absence of Smad3 did not impair myostatin-dependent MuRF1 induction during skeletal muscle atrophy. Bearing in mind that myostatin signaling through ActRIIB activates both Smad2 and Smad3, the former, *i.e.* Smad2, may be responsible for overexpression of MuRF1 (29, 36). Nonetheless, the role of MuRF1 in promoting myostatin-mediated skeletal muscle wasting remains to be fully understood, because only about 20% of sarcomeric protein loss could be attributed to MuRF1 activity in C2C12 myotubes treated with myostatin (Fig. 3D). It is noteworthy to mention that dexamethasone, an effective synthetic glucocorticoid, promotes wasting in skeletal muscle exclusively through inducing MuRF1-dependent degradation of thick filaments (7), indicating that the mechanism(s) through

which procachectic molecules promote muscle wasting are numerous.

Based on the observations in this study, we propose a novel model whereby myostatin induces muscle wasting (Fig. 7). Myostatin binding to ActRIIB results in the activation of the canonical Smad3-signaling pathway. Activated Smad3 will induce the expression of FoxO1, which, upon dephosphorylation, translocates into the nucleus to regulate Atrogin-1 expression. Although MuRF1 is also overexpressed in response to myostatin, it is Atrogin-1 that induces the degradation of sarcomeric proteins. Decreased protein synthesis in myotubes challenged with myostatin could be due to the decreased activity of Akt. Evidence presented in this report also suggests that the loss of translation machinery accounts for depressed protein synthesis during myostatin-mediated muscle wasting.

Materials and Methods

Animal care

Mstn$^{-/-}$, Atrogin-1$^{-/-}$, Smad3$^{+/-}$ (C57BL/6) mice were gifts from Se-Jin Lee (The Johns Hopkins University, Baltimore, MD), Esther Latres (Regeneron Pharmaceuticals, Tarrytown, NY) and Walter Wahli (University of Lausanne, Lausanne, Switzerland) respectively. WT mice (C57BL/6) were obtained from the Centre for Animal Resources (National University of Singapore, Singapore). All experiments were performed according to the approved protocols of the institutional animal ethics committee (IACUC), Singapore. For primary myoblast culture, mice were killed just before the commencement of the experiment by CO_2 asphyxiation, according to IACUC rules and regulations.

Expression and purification of myostatin, soluble ActRIIB, and follistatin

Recombinant Myostatin was expressed in both prokaryotic and eukaryotic cells. Myostatin protein was expressed and purified from *E. coli* according to McFarlane *et al.* (24). Myostatin-expressing CHO cells were kindly gifted by Se-Jin Lee (Johns Hopkins University) and were grown as previously described (22). Myostatin expression was induced by adding 50 μM of $ZnSO_4$ to serum free DMEM-F12 media and incubated for an additional 24 h (22, 24). Media from control CHO cells and myostatin-expressing cells were collected and centrifuged at 5000 $\times$ *g* for 10 min, followed by filtration using a 0.2-μm membrane filter.

The cDNA of soluble ActRIIB (38) or Follistatin (Fstn) (39) was cloned into the pET-16b expression vector (Novagen, Madison, WI), according to standard molecular biology protocols. Soluble ActRIIB and follistatin were expressed and purified as previously described (24). Activity of recombinant myostatin, Soluble ActRIIB, and follistatin was assessed using a myoblast assay (40).

Cell culture and treatments

Primary myoblasts were isolated exactly as previously described (41). C2C12 myoblasts (American Type Culture Collection, Manassas, VA) were cultured and differentiated for 72 h, as described previously (41). Differentiated myotubes were treated with myostatin, expressed in either CHO cells or *E. coli*. The conditioned media from CHO cells, induced to express myostatin, were used at a concentration of 1 ml (10 ng) or 2 ml (20 ng) of conditioned media per 10 ml of differentiation media (DMEM + 2% horse serum) to treat myotubes. The concentration of myostatin in conditioned media was estimated by ELISA (Diagnostik, Bensheim, Germany). Recombinant myostatin purified from *E. coli* was used at a concentration of 5 μg/ml to induce myotubular atrophy. To antagonize myostatin signaling, soluble ActRIIB and Fstn were added at a 1:1 ratio together with recombinant myostatin. To block proteasome activity the inhibitors MG132 (Sigma, St. Louis, MO) and Epox (Sigma) were added at 10 μM and 100 nM respectively, 10 h before harvesting the cells.

Extraction of RNA and real time qPCR

RNA was isolated from muscle and myotubes using TRIZOL reagent (Invitrogen, Carlsbad, CA), and cDNA was synthesized using the iScript system (Bio-Rad Laboratories, Inc., Hercules, CA), according to the manufacturer's instructions. Real-time PCR was performed using the CFX96 Real-Time system (Bio-Rad). Each real-time PCR (20 μl) contained 2 μl of 5 times diluted cDNA, 10 μl of 2$\times$ SsoFast Evagreen (Bio-Rad) and primers at a final concentration of 200 nM. All reactions were performed using the following thermal cycle conditions: 98 C for 3 min followed by 45 cycles of a three-step reaction, denaturation at 98 C for 3 sec, annealing at 60 C for 20 sec, followed by a melting curve from 60 to 95 C in 5-sec increments of 0.5 C to ensure amplification specificity. Transcript levels of target gene were normalized with *Gapdh*. Relative fold change in expression was calculated using the $\Delta\Delta$CT method. The sequence of the primers used in this manuscript is available upon request. All oligos pertaining to this study was purchased from Sigma Aldrich (Singapore).

Immunoblotting

Myoblasts and myotubes were resuspended in protein lysis buffer [50 mM Tris, (pH 7.5), 250 mM NaCl, 5 mM EDTA, 0.1% NP-40, Complete protease inhibitor cocktail (Roche, Indianapolis, MN), 2 mM NaF, 1 mM Na_3V0_4, and 1 mM phenylmethylsulfoxide (PMSF)], incubated for 15 min and then centrifuged at 12,000 rpm for 10 min. Supernatant was considered as the soluble fraction, and the pellet was referred to as the "insoluble" fraction, rich in sarcomeric proteins. The insoluble fraction was further processed according to protocol from Clarke *et al.* (7). Proteins were quantified using Bradford reagent (Bio-Rad). A total of 15 μg of each protein lysate was subjected to SDS-PAGE, using a 4–12% precast gel (Invitrogen), and the proteins were transferred to nitrocellulose membrane. The membrane was then blocked overnight at 4 C in 5% milk in 1$\times$ Tris-buffered saline-Tween 20 (TBST), and then incubated with primary antibodies for 3 h with 5% milk in 1$\times$ TBST. The membrane was washed in 1$\times$ TBST for 5 min (five times), and then incubated with either goat antimouse IgG-horseradish peroxidase (HRP) conjugate or goat antirabbit IgG-HRP conjugate

in blocking buffer for 1 h at room temperature. The washes were repeated, before HRP activity was detected using Western Lightning Chemiluminescence Reagent Plus (PerkinElmer, Boston, MA). The developed films were scanned and analyzed using Quantity One imaging software (Bio-Rad). Information pertaining to the antibodies is available in Supplemental Table 1.

Tandem affinity purification (TAP), coimmunoprecipitation

The Atrogin-1 (muscle atrophy F-box) cDNA was PCR amplified and cloned into pZome1C and pZome1N (Euroscraf, Germany) using standard molecular biological techniques with the following primers. C-terminal Atrogin-1: Forward primer, GGATCCATGCCGTTCCTT; reverse, GGATCCGAACTTGA ACAAATTGA; N-terminal-Atrogin-1: Forward, GAATTCAT GCCGTTCCTTG; reverse, GAATTCTCAGAACTTGAACA AATTGA. The recombinant plasmid was stably transfected into C2C12 myoblasts as described previously (24). C2C12 stably expressing Atrogin-1 were differentiated into myotubes and treated with 5 μg/ml myostatin (vehicle or control) for 24 h before protein extraction. Protein (5 mg) was subjected to tandem affinity purification according to protocol described previously (42–44). For coimmunoprecipitation studies, protein extracts from myostatin-treated C2C12 myotubes that stably express Atrogin-1 (as described above) were incubated with IgG-Agarose (Sigma) and the complex was purified as described previously (43). The immunoprecipitated complex was separated on 4–12% NuPAGE gels (Invitrogen) and transferred on to nitrocellulose membrane. Immunoblot was performed using a pan-Myh-specific antibody (24).

Measuring protein synthesis in C2C12 myotubes

Total protein synthesis was assessed through quantifying the amount of [^{3}H]tyrosine incorporation in C2C12 myotube cultures as described previously (45). C2C12 myotubes were treated with or without Mstn for 24 h. The myotubes were incubated with media containing 5 μCi/ml [^{3}H]tyrosine for 2 h. These samples were analyzed for total radioactivity incorporation and protein concentration using a scintillation counter (PerkinElmer) and Bradford assay, respectively. Results were expressed as disintegrations per minute per milligram of protein, normalized to the control. The experiment was repeated four times in duplicate.

Measuring protein degradation in C2C12 myotubes

C2C12 myotubes were incubated with 5 μCi/ml [^{3}H]tyrosine for 36 h to label cellular proteins (46). The media were then switched to the chase media containing 2 mM of unlabeled tyrosine and incubated for 2 h. Myotubes were then incubated with fresh chase media containing recombinant myostatin or MG132 or a combination thereof for 12 and 24 h. The media were collected at different intervals and precipitated with 10% trichoroacetic acid and centrifuged at 12,000 rpm for 10 min at 4 C. The acid-soluble radioactivity was measured using a scintillation counter (PerkinElmer). Radioactivity reflects the amount of prelabeled protein that was degraded, and it was expressed as a percentage of the total radioactivity initially incorporated. This experiment was repeated four times with duplicates, and values are represented as mean ± SD.

In vitro ubiquitination

In vitro ubiquitination was performed according to the previously described protocol (7). Briefly, 125 nM E1 (Boston Biochem, Inc); 4 μM UbcH5c (Boston Biochem, Inc.); 5 mM His6-biotin-hUB (Boston Biochem); 20, 30 or 50 nM GST-hAtrogin-1 (Abnova, Inc, Taipei, Taiwan); and 1 μM Myh or Myh complex (Sigma) was added to the reaction buffer [50 mM HEPES (pH 7.5)] containing 5 mM Mg-ATP solution (Sigma) and 0.6 mM dithiothreitol. All reactions were carried out for 1 h at room temperature and stopped by the addition of NuPAGE LDS sample buffer (Invitrogen). Proteins were then denatured by heating at 95 C and resolved on 4–12% Bis-Tris gels with 1× 2-(N-morpholino)ethanesulfonic acid SDS running buffer (Invitrogen) and transferred to nitrocellulose membranes for immunoblotting with anti-Ub antibody.

shRNA cloning, transfection, and stable cell line selection

Two different short-hairpin sequences were designed for each gene Atrogin-1, MuRF1 and Smad3 with high specificity, using the online software RNAi finder and Converter, available at the Applied Biosystems website (http://www.ambion.com/techlib/misc/siRNA_finder.html, and http://www.ambion.com/techlib/misc/psilencer_converter.html). The sequences of the shRNA oligos are available in Supplemental Table 2. Oligos were ligated into the *pSilencer* vector according to protocol recommended by the manufacturer (Applied Biosystems, Foster City, CA). Vectors containing correctly orientated, mutation-free short hairpin oligos were selected by sequencing. Vectors were transfected into C2C12 myoblasts using the previously described protocol (41). Negative control cells (with nonspecific shRNA expression) were generated simultaneously under the same conditions as mentioned above.

Measurement of myotube area

Myotubes were stained with hematoxylin and eosin and images were acquired using the Leica DM60000 B microscope (Leica Corp., Deerfield, IL). Myotubes containing more than or equal to three nuclei were considered for myotube area measurement. The myotube area was measured using the Image pro plus software and represented as μm^2. The graph was plotted by taking the average myotube area, and values are represented as mean ± SD.

Statistical analysis

One-way ANOVA and Student's *t* test were used for statistical significance measurement. The *P* values of $P < 0.05$ (*), $P < 0.01$ (**), and $P < 0.001$ (***) were considered as significant. *Error bar* represents mean of ±SD.

Acknowledgments

We thank Se-Jin Lee and Walter Wahli (University of Lausanne, Lausanne, Switzerland) for gifting the myostatin and Smad3 knockout mice, respectively. Further thanks to Esther Latres (Regeneron Pharmaceuticals) for providing the Atrogin-1 knockout mice and Atrogin-1 and MuRF1 antibodies used in the present study. We thank Developmental Studies Hybridoma

Bank for providing antibodies and Isuru Wijesoma (School of Biological Sciences, Nanyang Technological University, Singapore) for invaluable discussions and comments on the manuscript.

Address all correspondence and requests for reprints to: Ravi Kambadur, School of Biological Sciences, 60 Nanyang Drive, Nanyang Technological University, Singapore 637551. E-mail: kravi@ntu.edu.sg.

This work was supported by grants from the Ministry of Education, Singapore, and fellowship support from Nanyang Technological University (to S.L.).

Disclosure Summary: The authors declare no conflict of interest.

References

1. **Tisdale MJ** 2009 Mechanisms of cancer cachexia. Physiol Rev 89: 381–410
2. **Evans WJ** 2010 Skeletal muscle loss: cachexia, sarcopenia, and inactivity. Am J Clin Nutr 91:1123S–1127S
3. **Csibi A, Leibovitch MP, Cornille K, Tintignac LA, Leibovitch SA** 2009 MAFbx/Atrogin-1 controls the activity of the initiation factor eIF3-f in skeletal muscle atrophy by targeting multiple C-terminal lysines. J Biol Chem 284:4413–4421
4. **Csibi A, Tintignac LA, Leibovitch MP, Leibovitch SA** 2008 eIF3-f function in skeletal muscles: to stand at the crossroads of atrophy and hypertrophy. Cell Cycle 7:1698–1701
5. **Bodine SC, Latres E, Baumhueter S, Lai VK, Nunez L, Clarke BA, Poueymirou WT, Panaro FJ, Na E, Dharmarajan K, Pan ZQ, Valenzuela DM, DeChiara TM, Stitt TN, Yancopoulos GD, Glass DJ** 2001 Identification of ubiquitin ligases required for skeletal muscle atrophy. Science 294:1704–1708
6. **Gomes MD, Lecker SH, Jagoe RT, Navon A, Goldberg AL** 2001 Atrogin-1, a muscle-specific F-box protein highly expressed during muscle atrophy. Proc Natl Acad Sci USA 98:14440–14445
7. **Clarke BA, Drujan D, Willis MS, Murphy LO, Corpina RA, Burova E, Rakhilin SV, Stitt TN, Patterson C, Latres E, Glass DJ** 2007 The E3 Ligase MuRF1 degrades myosin heavy chain protein in dexamethasone-treated skeletal muscle. Cell Metab 6:376–385
8. **Cohen S, Brault JJ, Gygi SP, Glass DJ, Valenzuela DM, Gartner C, Latres E, Goldberg AL** 2009 During muscle atrophy, thick, but not thin, filament components are degraded by MuRF1-dependent ubiquitylation. J Cell Biol 185:1083–1095
9. **Krawiec BJ, Frost RA, Vary TC, Jefferson LS, Lang CH** 2005 Hindlimb casting decreases muscle mass in part by proteasome-dependent proteolysis but independent of protein synthesis. Am J Physiol Endocrinol Metab 289:E969–E980
10. **Schakman O, Gilson H, Kalista S, Thissen JP** 2009 Mechanisms of muscle atrophy induced by glucocorticoids. Horm Res 72(Suppl 1):36–41
11. **Testelmans D, Crul T, Maes K, Agten A, Crombach M, Decramer M, Gayan-Ramirez G** 2010 Atrophy and hypertrophy signaling in the diaphragm of patients with COPD. Eur Respir J 35:549–556
12. **Chen Y, Cao L, Ye J, Zhu D** 2009 Upregulation of myostatin gene expression in streptozotocin-induced type 1 diabetes mice is attenuated by insulin. Biochem Biophys Res Commun 388:112–116
13. **Léger B, Senese R, Al-Khodairy AW, Dériaz O, Gobelet C, Giacobino JP, Russell AP** 2009 Atrogin-1, MuRF1, and FoXO, as well as phosphorylated GSK-3β and 4E-BP1 are reduced in skeletal muscle of chronic spinal cord-injured patients. Muscle Nerve 40:69–78
14. **Mittal A, Bhatnagar S, Kumar A, Lach-Trifilieff E, Wauters S, Li H, Makonchuk DY, Glass DJ, Kumar A** 2010 The TWEAK-Fn14 system is a critical regulator of denervation-induced skeletal muscle atrophy in mice. J Cell Biol 188:833–849
15. **Sandri M, Sandri C, Gilbert A, Skurk C, Calabria E, Picard A, Walsh K, Schiaffino S, Lecker SH, Goldberg AL** 2004 Foxo transcription factors induce the atrophy-related ubiquitin ligase atrogin-1 and cause skeletal muscle atrophy. Cell 117:399–412
16. **Latres E, Amini AR, Amini AA, Griffiths J, Martin FJ, Wei Y, Lin HC, Yancopoulos GD, Glass DJ** 2005 Insulin-like growth factor-1 (IGF-1) inversely regulates atrophy-induced genes via the phosphatidylinositol 3-kinase/Akt/mammalian target of rapamycin (PI3K/Akt/mTOR) pathway. J Biol Chem 280:2737–2744
17. **Xu Q, Wu Z** 2000 The insulin-like growth factor-phosphatidylinositol 3-kinase-Akt signaling pathway regulates myogenin expression in normal myogenic cells but not in rhabdomyosarcoma-derived RD cells. J Biol Chem 275:36750–36757
18. **McPherron AC, Lee SJ** 1997 Double muscling in cattle due to mutations in the myostatin gene. Proc Natl Acad Sci USA 94:12457–12461
19. **Kambadur R, Sharma M, Smith TP, Bass JJ** 1997 Mutations in myostatin (GDF8) in double-muscled Belgian Blue and Piedmontese cattle. Genome Res 7:910–916
20. **Schuelke M, Wagner KR, Stolz LE, Hübner C, Riebel T, Kömen W, Braun T, Tobimatsu JF, Lee SJ** 2004 Myostatin mutation associated with gross muscle hypertrophy in a child. N Engl J Med 350:2682–2688
21. **McPherron AC, Lawler AM, Lee SJ** 1997 Regulation of skeletal muscle mass in mice by a new TGF-β superfamily member. Nature 387:83–90
22. **Zimmers TA, Davies MV, Koniaris LG, Haynes P, Esquela AF, Tomkinson KN, McPherron AC, Wolfman NM, Lee SJ** 2002 Induction of cachexia in mice by systemically administered myostatin. Science 296:1486–1488
23. **Durieux AC, Amirouche A, Banzet S, Koulmann N, Bonnefoy R, Pasdeloup M, Mouret C, Bigard X, Peinnequin A, Freyssenet D** 2007 Ectopic expression of myostatin induces atrophy of adult skeletal muscle by decreasing muscle gene expression. Endocrinology 148:3140–3147
24. **McFarlane C, Plummer E, Thomas M, Hennebry A, Ashby M, Ling N, Smith H, Sharma M, Kambadur R** 2006 Myostatin induces cachexia by activating the ubiquitin proteolytic system through an NF-κB-independent, FoxO1-dependent mechanism. J Cell Physiol 209:501–514
25. **Trendelenburg AU, Meyer A, Rohner D, Boyle J, Hatakeyama S, Glass DJ** 2009 Myostatin reduces Akt/TORC1/p70S6K signaling, inhibiting myoblast differentiation and myotube size. Am J Physiol Cell Physiol 296:C1258–C1270
26. **Zhou X, Wang JL, Lu J, Song Y, Kwak KS, Jiao Q, Rosenfeld R, Chen Q, Boone T, Simonet WS, Lacey DL, Goldberg AL, Han HQ** 2010 Reversal of cancer cachexia and muscle wasting by ActRIIB antagonism leads to prolonged survival. Cell 142:531–543
27. **Lee SJ, Reed LA, Davies MV, Girgenrath S, Goad ME, Tomkinson KN, Wright JF, Barker C, Ehrmantraut G, Holmstrom J, Trowell B, Gertz B, Jiang MS, Sebald SM, Matzuk M, Li E, Liang LF, Quattlebaum E, Stotish RL, Wolfman NM** 2005 Regulation of muscle growth by multiple ligands signaling through activin type II receptors. Proc Natl Acad Sci USA 102:18117–18122
28. **Walsh S, Metter EJ, Ferrucci L, Roth SM** 2007 Activin-type II receptor B (ACVR2B) and follistatin haplotype associations with muscle mass and strength in humans. J Appl Physiol 102:2142–2148
29. **Amthor H, Nicholas G, McKinnell I, Kemp CF, Sharma M, Kambadur R, Patel K** 2004 Follistatin complexes myostatin and antagonises myostatin-mediated inhibition of myogenesis. Dev Biol 270: 19–30
30. **Tawa Jr NE, Odessey R, Goldberg AL** 1997 Inhibitors of the proteasome reduce the accelerated proteolysis in atrophying rat skeletal muscles. J Clin Invest 100:197–203

31. **Langley B, Thomas M, Bishop A, Sharma M, Gilmour S, Kambadur R** 2002 Myostatin inhibits myoblast differentiation by down-regulating MyoD expression. J Biol Chem 277:49831–49840
32. **Amirouche A, Durieux AC, Banzet S, Koulmann N, Bonnefoy R, Mouret C, Bigard X, Peinnequin A, Freyssenet D** 2009 Down-regulation of Akt/mammalian target of rapamycin signaling pathway in response to myostatin overexpression in skeletal muscle. Endocrinology 150:286–294
33. **McFarlane C, Sharma M, Kambadur R** 2008 Myostatin is a pro-cachectic growth factor during postnatal myogenesis. Curr Opin Clin Nutr Metab Care 11:422–427
34. **Lagirand-Cantaloube J, Offner N, Csibi A, Leibovitch MP, Batonnet-Pichon S, Tintignac LA, Segura CT, Leibovitch SA** 2008 The initiation factor eIF3-f is a major target for atrogin1/MAFbx function in skeletal muscle atrophy. EMBO J 27:1266–1276
35. **Lagirand-Cantaloube J, Cornille K, Csibi A, Batonnet-Pichon S, Leibovitch MP, Leibovitch SA** 2009 Inhibition of atrogin-1/MAFbx mediated MyoD proteolysis prevents skeletal muscle atrophy in vivo. PLoS One 4:e4973
36. **Sartori R, Milan G, Patron M, Mammucari C, Blaauw B, Abraham R, Sandri M** 2009 Smad2 and 3 transcription factors control muscle mass in adulthood. Am J Physiol Cell Physiol 296:C1248–C1257
37. **Amthor H, Huang R, McKinnell I, Christ B, Kambadur R, Sharma M, Patel K** 2002 The regulation and action of myostatin as a negative regulator of muscle development during avian embryogenesis. Dev Biol 251:241–257
38. **Lee SJ, McPherron AC** 2001 Regulation of myostatin activity and muscle growth. Proc Natl Acad Sci USA 98:9306–9311
39. **Hill JJ, Davies MV, Pearson AA, Wang JH, Hewick RM, Wolfman NM, Qiu Y** 2002 The myostatin propeptide and the follistatin-related gene are inhibitory binding proteins of myostatin in normal serum. J Biol Chem 277:40735–40741
40. **McCroskery S, Thomas M, Maxwell L, Sharma M, Kambadur R** 2003 Myostatin negatively regulates satellite cell activation and self-renewal. J Cell Biol 162:1135–1147
41. **McFarlane C, Hennebry A, Thomas M, Plummer E, Ling N, Sharma M, Kambadur R** 2008 Myostatin signals through Pax7 to regulate satellite cell self-renewal. Exp Cell Res 314:317–329
42. **Tsai A, Carstens RP** 2006 An optimized protocol for protein purification in cultured mammalian cells using a tandem affinity purification approach. Nat Protoc 1:2820–2827
43. **Woodcock SA, Jones RC, Edmondson RD, Malliri A** 2009 A modified tandem affinity purification technique identifies that 14-3-3 proteins interact with Tiam1, an interaction which controls Tiam1 stability. J Proteome Res 8:5629–5641
44. **Bürckstümmer T, Bennett KL, Preradovic A, Schütze G, Hantschel O, Superti-Furga G, Bauch A** 2006 An efficient tandem affinity purification procedure for interaction proteomics in mammalian cells. Nat Methods 3:1013–1019
45. **Driscoll J, Goldberg AL** 1990 The proteasome (multicatalytic protease) is a component of the 1500-kDa proteolytic complex which degrades ubiquitin-conjugated proteins. J Biol Chem 265:4789–4792
46. **Hershko A** 1988 Ubiquitin-mediated protein degradation. J Biol Chem 263:15237–15240